Generation of Bessel beam arrays through Dammann gratings

Pascuala García-Martínez,[1,*] María M. Sánchez-López,[2] Jeffrey A. Davis,[3] Don M. Cottrell,[3] David Sand,[3] and Ignacio Moreno[4]

[1]Departament d'Òptica, Universitat de València, 46100 Burjassot, Spain

[2]Instituto de Bioingeniería, Universidad Miguel Hernández, 03202 Elche, Spain

[3]Physics Department, San Diego State University, California, USA

[4]Departamento de Ciencia de Materiales, Óptica y Tecnología Electrónica, Universidad Miguel Hernández, 03202 Elche, Spain

*Corresponding author: pascuala.garcia@uv.es

Received 8 September 2011; accepted 31 October 2011;
posted 14 November 2011 (Doc. ID 154329); published 15 March 2012

In this work we apply the Dammann grating concept to generate an equal-intensity square array of Bessel quasi-free diffraction beams that diverge from a common center. We generate a binary phase mask that combines the axicon phase with the phase of a Dammann grating. The procedure can be extended to include vortex spiral phases that generate an array of optical pipes. Experimental results are provided by means of a twisted nematic liquid crystal display operating as a binary π phase spatial light modulator. © 2012 Optical Society of America

OCIS codes: 050.1380, 050.1950, 120.5060, 070.6120.

1. INTRODUCTION

Bessel beams are optical beams with a Bessel function electric-field profile that can propagate without diffraction. They were introduced by Durnin who looked at Whitaker's solutions of the Helmholtz equation and verified that particular solutions of the Bessel type were theoretically independent of the propagation direction [1]. In practice, ideal Bessel beams are not strictly realizable, but quasi-Bessel beams can be experimentally generated, which possess the focusing properties over a finite distance [2]. Bessel beams have prospective applications, such as optical alignment, interconnection [2], and promotion of free electron laser gain [3].

Bessel beams can be generated in a number of ways. In the original contribution, Durnin *et al* [4] presented a simple optical system consisting of a narrow annular slit and a lens placed one focal length away. In [5], McLeod proposed the axicon (the conical lens), which now is the most usual method to generate Bessel beams [6]. This refractive element produces a line focus from an incident collimated light, rather than the point focus from a usual lens. This line focus can be approximately considered to be a zero order Bessel beam that has a finite propagation distance. Other efficient methods of creating Bessel beams are based on diffractive optical elements (DOEs) that reproduce the optical behavior of the axicon, either with static computer generated holograms [7] or by means of controlled devices such a spatial light modulators (SLMs) [8–12]. Note that the source and the propagation angle of the nondiffracting beam relative to the optical axis can be altered by combining gratings onto the axicon pattern or by shifting the origin of the pattern [7–8,11–12].

Binarized versions of these diffractive elements are commonly used due to the difficulty to produce multilevel DOE's [8–13]. The phase binarization of

1559-128X/12/091375-07$15.00/0

diffractive axicons implies that the optical response of the refractive conical lens is reproduced in the first-order diffraction component, with a maximum diffraction efficiency of 40.5% relative to the energy of the incoming beam, a situation that is obtained when the phase difference between the two levels in the binary phase mask is π radians. As mentioned earlier, the propagation angle of the nondiffracting beam can be altered by combining a diffraction grating onto the axicon pattern [8,11–12], but again the diffraction efficiency is limited by the grating efficiency.

Dammann gratings represent another group of specially designed binary $(0, \pi)$ phase diffraction gratings. They are designed to create a diffraction pattern where the intensities of the diffracted spots are equal for a given number of orders [13]. This is accomplished by dividing each grating period into different segments having precise transition points. A useful set of transition points required for generating a desired number of diffracted orders can be found in [14]. Recently, an approach was demonstrated for extending this Dammann grating concept to more general phase structures [15], which has been applied to generate three-dimensional arrays of focusing spots [16].

In this work, we report on the combination of a diffractive axicon with a Dammann grating structure, in order to create a square array of equally intense Bessel beams that diverge from a common center and remain almost diffraction free over a certain range. Our approach is extremely simple by implementing either fixed or programmable optical elements. It uses existing tabulated parameters for the Dammann grating [14], thus avoiding any time consuming algorithms. The designed axicon Dammann grating can be further combined with a spiral phase pattern in order to transform the array of diverging Bessel beams into an array of vortex Bessel beams, which create optical pipes over the same range. This system can be very useful in all types of applications that require multiple large-focusing beams like optical tweezers, where a large number of equal intense optical traps are needed, optical processors for parallel communication or wavefront sensing, where again it is highly desirable to generate an array of multiple beams that exhibits maximum localization in space and time, as well as for precision alignment systems, laser machining or laser surgery among others.

The paper is organized with four sections. After this introduction, Section 2 reviews the theory first for the axicon including vortex-generating masks and the effect of the phase binarization, and then for Dammann diffraction gratings. The two ideas are then combined into the axicon Dammann grating. Section 3 includes experimental results for all these masks obtained using a twisted nematic liquid crystal display (TN-LCD) operating in a π binary phase-only modulation configuration. Finally, Section 4 includes the conclusions of the work.

2. BINARY AXICONS AND DAMMANN GRATINGS

A. Binary Axicons

The classical linear axicon phase function is given by

$$g(r) = \exp\left[i\phi(r)\right] = \exp(-i2\pi r/r_0), \tag{1}$$

where $r = \sqrt{x^2 + y^2}$ is the radial coordinate and r_0 is an adjustable control parameter that controls the diameter of the Bessel function beam. The phase function $\phi(r) = 2\pi r/r_0$ creates a beam with an approximate Bessel function profile that stays constant over a distance $z_{\max} = Dr_0/2\lambda$, where D is the width of the phase mask and λ is the wavelength of the illuminating light beam [8]. When this pattern is encoded onto a diffractive pixelated SLM, then $r^2 = (i^2 + j^2)\Delta^2$, where (i,j) are integers identifying each pixel, and Δ is the pixel spacing (assumed to be identical in the x and y directions). If the period of the axicon is selected to be $r_0 = p\Delta$ (where the Nyquist limit is $p = 2$), and the width D is expressed as $D = M\Delta$, where M is the number of pixels in the SLM, then the maximum range of the Bessel beam can be expressed simply as

$$z_{\max} = \frac{pM\Delta^2}{2\lambda}. \tag{2}$$

For distances larger than $z_{\max}$, the focusing property of the axicon is lost.

If the linear phase function in Eq. (1) is encoded onto a binary phase-only SLM, the binarized version $g'(r) = \mathbf{BIN}[g(r)]$ can be expanded in a Fourier series as

$$g'(r) = \sum_{m=-\infty}^{+\infty} c_m \exp(-i2\pi mr/r_0), \tag{3}$$

with the Fourier coefficients

$$c_m = \int_0^{r_0} g'(r) \exp(+i2\pi mr/r_0)\mathrm{d}r. \tag{4}$$

Equation (3) shows that the binarized axicon can be viewed as the superposition of different harmonic terms that take the form of other axicons with parameters $r_{0m} = r_0/m$, each one weighted by the corresponding Fourier coefficient c_m. The term $m = 1$ corresponds to the linear axicon. Positive harmonic components with order m produce narrower Bessel beams with shorter ranges given by [9]

$$z_{\max}(m) = \frac{1}{m}\frac{pM\Delta^2}{2\lambda}. \tag{5}$$

The term $m = 0$ corresponds to the amount of light that traverses the diffractive element unaffected, while negative harmonic components corresponds to diverging axicons that create virtual Bessel beams.

In the case of a regular phase binarization [phases 0 and π are respectively assigned to phase ranges $(0, \pi)$ and $(\pi, 2\pi)$], the Fourier coefficients in Eq. (3) are $c_m = 2i/m\pi$ for odd values of m, and vanish for all even orders, including the DC term ($m = 0$). Therefore, orders $m = \pm 1$ each carry 40.5% of the total energy, while the rest of the energy is split into the other odd harmonic components [9]. Note that these higher harmonic components will have shorter ranges from Eq. (5).

In this situation, for ranges from the phase axicon grating that are larger than the maximum range for the higher-order harmonic axicon (in this case for $m = 3$, where $z_{\max}(m = 3) = pM\Delta^2/6\lambda$), their contributions can be neglected and the generated light beam can be approximated by the Bessel beam of the first-order positive axicon, with 40.5% of the total power.

Higher order Bessel beams can also be obtained by adding a spiral phase to the axicon phase [9–10], to create a vortex axicon phase plate. The phase function in Eq. (1) is modified to

$$g(r,\theta) = \exp\left[-i\left(\frac{2\pi r}{r_0} + \ell\theta\right)\right], \tag{6}$$

where θ is the azimuth angle, and where ℓ denotes the topological charge. The resulting vortex-creating axicon produces a nondiffracting beam corresponding to the J_ℓ Bessel function that, when $\ell \neq 0$, shows a dark center and a surrounding ring of light whose diameter depends on the topological charge, and with the same focusing range as the original nondiffracting beam.

Note that the effect of the phase binarization $g'(r,\theta) = \mathbf{BIN}[g(r,\theta)]$ in this case leads to a Fourier series expansion in the form

$$g'(r,\theta) = \sum_{m=-\infty}^{+\infty} c_m \exp(-i2\pi m r/r_0)\exp(-im\ell\theta). \tag{7}$$

This shows that the binarized version of the vortex axicon produces the superposition of converging and diverging harmonic components corresponding to vortex axicons with parameters $r_{0m} = r_0/m$ and $\ell_m = m\ell$. Note again that these higher harmonic components will have shorter ranges from Eq. (5).

Figure 1 shows the characteristics of these binarized axicons. We show an incident ray at a given radius that is diffracted by the diffractive axicon. We see the two positive orders that coincide at different axial positions. The first order intersects the optical axis at a farther distance than the second order and produces a beam having a smaller radius dependent on $r_{0m} = r_0/m$, but a larger diameter depending on the size of the charge $\ell_m = m\ell$. The negative orders correspond to diverging axicons that create virtual Bessel beams at negative propagation distances. The rays generated by these diverging axicons diverge and do not contribute to the output intensity

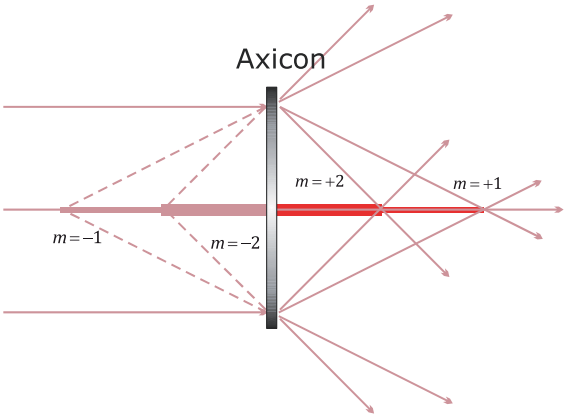

Fig. 1. (Color online) Schematic of the effects due to the binarization of the axicon phase profile. Multiple orders generate multiple axicon terms.

at the region of focusing of the main converging axicon component ($m = +1$).

Thus, if we consider distances from the binary phase grating that are larger than the ranges for the higher-order harmonic axicons, their contributions can be neglected and the generated light beam effectively reproduces the J_ℓ Bessel beam, with 40.5% of the total incoming power.

Normally, these beams propagate along the optical axis. However the propagation direction can be altered by encoding a blaze diffraction grating having a period d_0 onto the axicon phase [7,10]. As a result, the nondiffracting beam travels along an angle α to the optical axis that depends on the period d_0 of the grating as $\sin\alpha = \lambda/d_0$. The generating axicon pattern is now written as

$$g(r,\theta) = \exp(-i2\pi r/r_0)\exp(i\ell\theta)\exp(i2\pi x/d_0). \tag{8}$$

At this point, the binarization process can produce different results depending on the order in which the various functions are binarized [15–16]. We consider the case where the grating function is binarized and multiplied by the binarized axicon function from Eq. (7), i.e., $g'(r,\theta) = \mathbf{BIN}[\exp(-i2\pi r/r_0)\exp(i\ell\theta)]\times \mathbf{BIN}[\exp(i2\pi x/d_0)]$. In this case, we obtain the following Fourier series expansion as

$$g'(r,\theta) = \left[\sum_{m=-\infty}^{+\infty} c_m \exp(-i2\pi m r/r_0)\exp(-im\ell\theta)\right] \times \left[\sum_{n=-\infty}^{+\infty} c_n \exp(i2\pi n x/d_0)\right]. \tag{9}$$

Again if we use the regular $(0,\pi)$ binarization process for the axicon pattern, the dominant Fourier coefficients are the $m = \pm 1$ that each carry 40,5% of the total energy, while the rest of the energy is split into the other odd harmonic components. For the first summation, the $m = -1$ order for the axicon is diverging as shown in Fig. 1. Consequently the left hand

series produces basically the single Bessel function beam with a charge ℓ. The right hand sum produces a series of beams that travel at angles of $n\alpha$ relative to the optical axis. Again if we use the regular $(0, \pi)$ binarization process for the grating, the grating dominant Fourier coefficients are the $n = \pm 1$ components that each carry 40.5% of the total energy from the axicon $m = +1$ order (or 16.4% of the incident energy).

The result in this case would be a series of axicons having identical charges ℓ that are diffracting along a set of directions $n\alpha$ whose strengths are determined by the coefficients c_n. However using the normal binarization process, we would only see the $m = +1$ order for the axicon and the $n = \pm 1$ orders for the directions. These would produce two beams that diverge at angles $\pm\alpha$ relative to the optical axis. However the numbers and strengths of the diffracted orders are usually limited with the usual encoding techniques.

Next we consider the implications of utilizing Dammann gratings.

B. Dammann Gratings and Bessel Beams Arrays

Another area where binary phase SLM's have been employed is for the use of Dammann diffraction gratings. These are specially designed binary $(0, \pi)$ phase gratings that produce a diffraction pattern with a set of equally intense diffraction orders [13] where the values of the coefficients c_n are equal for a given set of orders. They are obtained by accurately selecting the transition points within a period (an extensive detail of the transition points for different numbers of diffraction orders can be found for instance in [14]). Two-dimensional arrays can be constructed by forming the product of two one-dimensional (1D) arrays.

So the basic idea is exactly the same as in Eq. (9). However by using a specially designed Dammann grating of order N, we can produce an array of N Bessel beams having different propagation angles with identical strengths. By constructing two dimensional Dammann gratings of order $N \times N$, we can produce a two dimensional array of diverging axicons with equal strengths. By combining the angular phase term $\ell\theta$, each of these axicons represent the higher order Bessel functions. The only change in the previous results is that the number of orders in Eq. (9) increases.

Figure 2 shows the process of generating these kinds of patterns. Figure 2(a) shows the diffractive pattern corresponding to a linear axicon with a period $p = 10$ pixels where the gray levels correspond to phase levels in the phase range $[0, 2\pi)$. Figure 2(b) shows the corresponding binary version where black and white denote phases 0 and π respectively. Figure 2(c) shows the binary version of the vortex axicon with period $r_0 = 10\Delta$ and topological charge $\ell = 16$. Figure 2(d) shows an example of a binary two dimensional Dammann grating designed to create an array of 4×4 equally intense diffraction orders. Here transition points have been applied at values

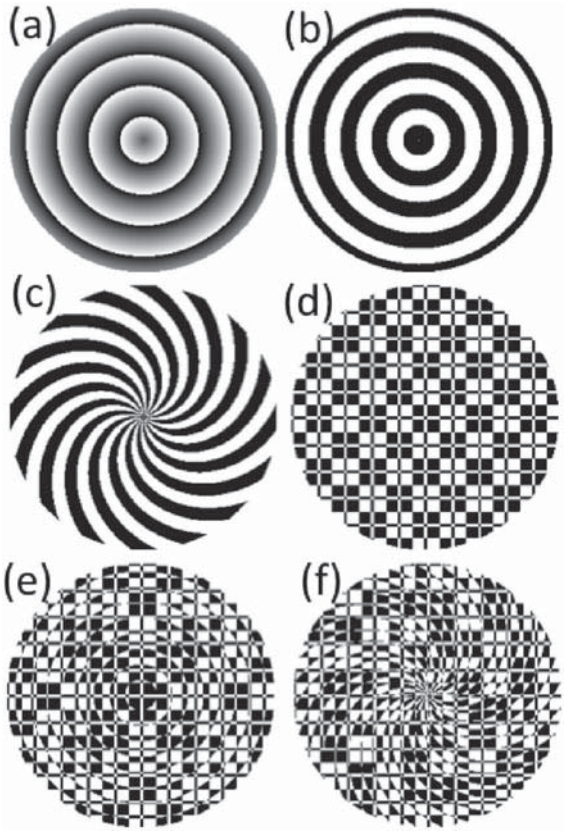

Fig. 2. Two dimensional (2D) binary phase patterns for (a) Linear axicon, (b) Binary axicon, (c) Binary vortex axicon, (d) 2D Dammann grating, (e) 2D Dammann axicon and (f) 2D Dammann vortex axicon.

0.22057, 0.44563, 0.5, 0,72057 and 0,94563 within a single period, as described in [14]. The period of the grating has been selected to be 35 pixels. This 2D grating has been obtained from the product of two orthogonal 1D gratings. Figures 2(e) and 2(f) show the resulting pattern after the multiplication of the patterns in Fig. 2(b) and 2(d) (the binary axicon and the Dammann grating), and the patterns in Fig. 2(c) and 2(d) (the binary vortex axicon and the Dammann grating), respectively. Note that all these are binary phase patterns, which therefore can be directly encoded onto a binary phase SLM. The phase levels must be adjusted to have a relative π phase difference to ensure the absence of the zero order DC term.

3. EXPERIMENTAL RESULTS

Experimental results were obtained using a CRL model XGA-3 twisted nematic liquid crystal display (TNLCD) having 1074 × 768 pixels and pixel spacing of $\Delta = 18$ μm, and an active area of 13 μm × 10 μm, thus having a fill factor $F \sim 40.1\%$. Note that the pixelated structure of the device adds and additional source of loss in the diffractive efficiency, that in the zero order is equal to $F^2 \sim 16.1\%$. The device is operated in the polarization average eigenvector configuration as described in [17], in order to act in a phase-only mode. We illuminated the SLM with a

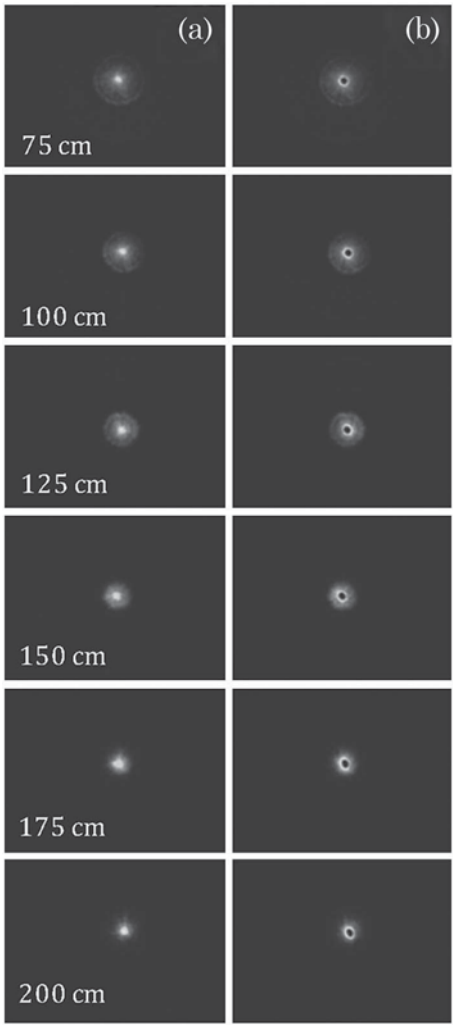

Fig. 3. Experimental patterns at various distances from the SLM for (a) the binary axicon [using the binary phase pattern from Fig. 2(b)], (b) the binary vortex axicon with charge $\ell = 16$ [using the binary phase pattern from Fig. 2(c)].

collimated 0.488 μm wavelength Ar ion laser beam, and examined the diffraction pattern formed by free propagation of distance z from the SLM. The binary phase masks were encoded with two appropriate gray levels so that the two regions show a relative phase shift of π radians. The corresponding diffraction pattern was captured with a CCD camera, (Basler, model scA1390-17fc, with 1392×1040 pixels), which was mounted on an adjustable stage so that the various focal plane structures could be recorded. Experimental results are shown next.

We first analyze the binary axicon and the binary vortex axicon, as shown in Figs. 2(b) and 2(c). They were selected with a period $r_0 = 10\Delta$, and the laser beam illuminates a circular area of the SLM with a diameter D of $M = 690$ pixels, thus leading to an expected value $z_{\max} \cong 230$ cm. Note that $z_{\max}$ for $m = 3$ (corresponding to the third harmonic component of the axicon), is approximately 76 cm. Thus, the first order ($m = 1$) harmonic component of the axicon is isolated in the distance from 76 to 230 cm from the SLM plane as shown schematically in Fig. 1. Figure 3 shows the experimentally captured diffraction patterns at various distances. At distances closer than $z = 75$ cm, overlapping interference effects between higher-order beams modify the shape of the Bessel function [9]. At larger distances the interference effects between the various orders of the axicon patterns are not seen, and the $m = 1$ nondiffracting Bessel beam is formed.

Note from Fig. 3 that, along the z-range, the sizes and the pattern of the intensity distributions near the center of the beam remain unchanged. The patterns for the regular binary axicons show a bright spot on axis, while the binary vortex axicons ($\ell = 16$) produce a nondiffracting beam with a null intensity at the center.

Next we analyzed the results for the array of Bessel beams generated when combining these phase patterns with the Dammann grating. We first selected a fixed plane in the middle of the focusing range, at distance $z = 175$ cm, and generated the phase mask that combines the 4×4 Dammann grating with a binary axicon. As pointed out before, the Dammann grating structure requires extremely accurate transition points within each period. The difficulty occurs when writing these structures onto a pixelated device because the transition points often do not coincide with the pixel structure. Consequently we conducted experiments to determine the best overall grating periods that allowed us to accurately encode these structures and choose periods that give, in our display, a set of equally intense diffracted orders. We obtained good results with a Dammann grating period of 35 pixels.

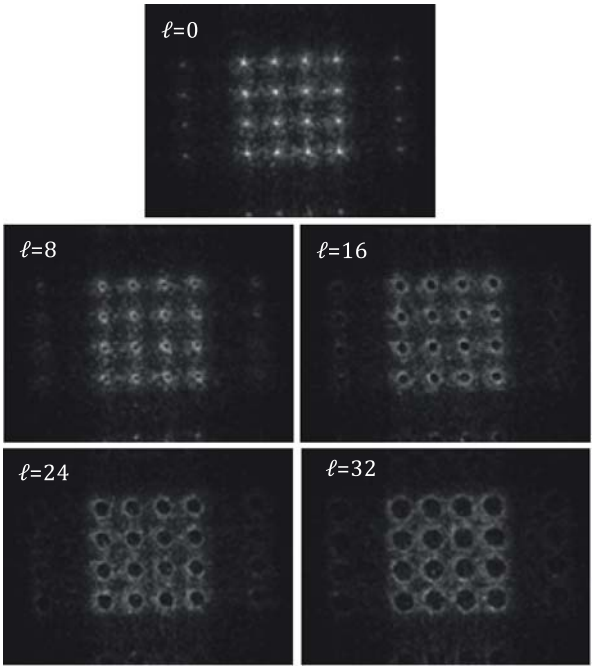

Fig. 4. Experimental patterns at distance of $z = 175$ cm for various Dammann vortex axicons with different values of the topological charge ℓ.

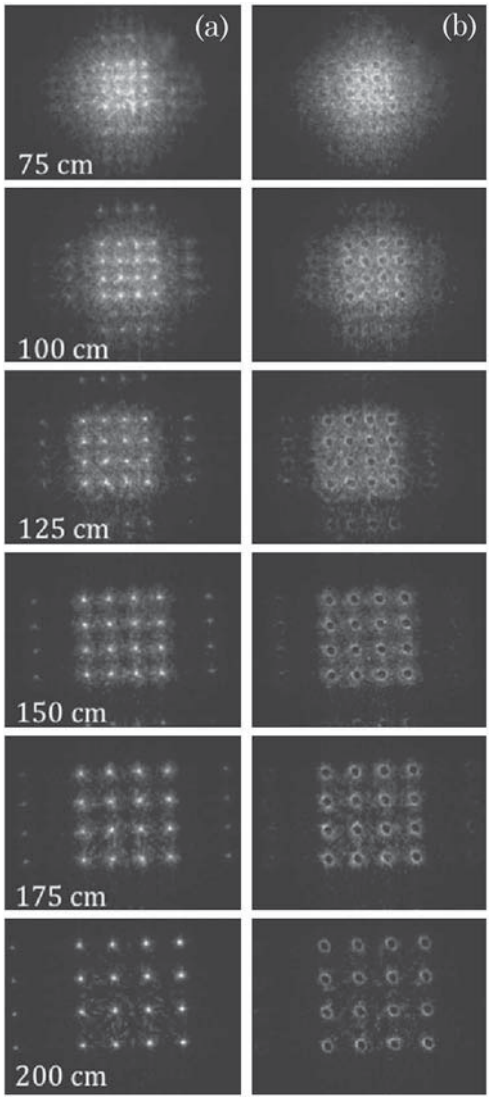

Fig. 5. Experimental patterns at various distances from the SLM for the (a) Dammann axicon using the binary phase pattern from Fig. 2(e), (b) Dammann vortex ($\ell = 16$) axicon using the binary phase pattern from Fig. 2(f).

The same Dammann grating was then combined with vortex axicons with different topological charges ($\ell = 0, 8, 16, 24, 32$). Note that the case $\ell = 0$ corresponds to the standard axicon. The corresponding experimental results are shown in Fig. 4. They probe the generation in this plane of a light pattern that shows the 4×4 set of beams with the desired characteristics. For $\ell = 0$ we can observe the generation of an array of 4×4 bright spots, characteristic of the Dammann grating. For higher values of ℓ, we observe how the structure of each of the 4×4 beams shows the dark spot in the center characteristic of the vortex beams. As expected, the diameter of the doughnut light beams increases as ℓ increases. We can observe that there exists a limitation to avoid overlapping between the adjacent beams that depends on the separation between the diverging Bessel beams and their diameters.

Finally we tested the range of distances where this 4×4 array of Bessel beams is maintained. We can expect that this range must be reduced due to the interference among the multiple versions of the Bessel beam generated by the Dammann grating. Figure 5 shows experimental results at the same distances as in Fig. 3, but obtained with the Dammann axicon and with the Dammann vortex axicon ($\ell = 16$) phase masks shown in Figs. 2(e) and 2(f) respectively. We can remarkably see how the 4×4 array of Bessel beams is effectively generated in the range from 125 to 200 cm from the SLM plane and that the size of the 4×4 array increases with distance. As mentioned earlier, the overlapping of the individual beams depends on the Dammann grating period, the charge of the vortices, and the observation distance. However, we confirm the generation of a large focusing region (close to 100 cm in this experiment) where a two dimensional array of Bessel beams can be generated, to produce a 4×4 array of line focus beams [Fig. 5(a)] or light pipes [Fig. 5(b)].

4. CONCLUSIONS

In summary, we have shown how to generate Dammann phase structures that produce a two dimensional array of diverging Bessel beams by a simple combination of standard Dammann diffraction gratings and diffractive versions of the axicon phase. Spiral phase patterns can also be added to easily generate higher order Bessel beam arrays. The technique is very simple to integrate, requires no computer optimization, and offers a great versatility in adjusting the number, spacing and order of the Bessel beams. The approach is entirely programmable since it uses patterns encoded onto a spatial light modulator. The technique might be suitable for applications including multiple testing and multialignment.

PGM, MMSL and IM acknowledge financial support from the Spanish Ministerio de Ciencia e Innovación (grant FIS2009-13955-C02-02) and Generalitat Valenciana (grant ACOMP/2010/112).

References

1. J. Durnin, "Exact solutions for nondiffracting beams I. The scalar theory," J. Opt. Soc. Am. A **4**, 651–654 (1987).
2. D. McGloin and K. Dholakia, "Bessel beams: diffraction in a new light," Contemp. Phys. **46**, 15–28 (2005).
3. D. Li, K. Imasaki, S. Miyamoto, S. Amano, and T. Mochizuki, "Conceptual design of Bessel beam cavity for free-electron laser," Int. J. Infrared Millim. Waves **27**, 165–171 (2006).
4. J. Durnin, J. J. Miceli Jr., and J. H. Eberly, "Diffraction free beams," Phys. Rev. Lett. **58**, 1499–1501 (1987).
5. J. H. McLeod, "The axicon: a new type of element," J. Opt. Soc. Am. **44**, 592–597 (1954).
6. G. Scott and M. McArdle, "Efficient generation of nearly diffraction-free beams using an axicon," Opt. Eng. **31**, 2640–2643 (1992).
7. A. Vasara, J. Turunen, and A. T. Friberg, "Realization of general nondiffracting beams with computer-generated holograms," J. Opt. Soc. Am. A **6**, 1748–1754 (1989).
8. J. A. Davis, J. Guertin, and D. M. Cottrell, "Diffraction-free beams generated with programmable spatial light modulators," Appl. Opt. **32**, 6368–6370 (1993).

9. J. A. Davis, E. Carcole, and D. M. Cottrell, "Nondiffractive interference patterns generated with programmable spatial light modulators," Appl. Opt. **35**, 599–602 (1996).
10. J. A. Davis, E. Carcole, and D. M. Cottrell, "Intensity and phase measurements of nondiffracting beams generated with a magneto optical spatial light modulator," Appl. Opt. **35**, 593–598 (1996).
11. J. A. Davis, E. Carcole, and D. M. Cottrell, "Range-finding by triangulation of nondiffracting beams," Appl. Opt. **35**, 2159–2161, (1996).
12. Z. Jaroszewicz, V. Climent, V. Durán, J. Lancis, A. Kolodziejczyk, A. Burvall, and A. T. Friberg, "Programmable axicon for variable inclination of the focal segment," J. Mod. Opt. **51**, 2185–2190 (2004).
13. H. Dammann and E. Klotz, "Coherent optical generation and inspection of two-dimensional periodic structures," Opt. Acta **24**, 505–515 (1977).
14. C. Zhou and L. Liu, "Numerical study of Dammann array illuminators," Appl. Opt. **34**, 5961–5969 (1995).
15. I. Moreno, J. A. Davis, D. M. Cottrell, N. Zhang, and X.-C. Yuan, "Encoding generalized phase functions on Dammann gratings," Opt. Lett. **35**, 1536–1538 (2010).
16. J. A. Davis, I. Moreno, J. L. Martínez, T. J. Hernández, and D. M. Cottrell, "Creating three-dimensional lattice patterns using programmable Dammann gratings," Appl. Opt. **50**, 3653–3657 (2011).
17. I. Moreno, J. L. Martínez, and J. A. Davis, "Two-dimensional polarization rotator using a twisted-nematic liquid crystal display," Appl. Opt. **46**, 881–887 (2007).